

Non-cyclic Geometric Phase due to Spatial Evolution in a Neutron Interferometric Setup

Stefan Filipp,^{1, 2, *} Yuji Hasegawa,^{1, †} Rudolf Loidl,² and Helmut Rauch¹

¹Atominstitut der Österreichischen Universitäten, Stadionallee 2, A-1020 Vienna, Austria

²Institut Laue Langevin, Boîte Postale 156, F-38042 Grenoble Cedex 9, France

We present a split-beam neutron interferometric experiment to test the non-cyclic geometric phase tied to the spatial evolution of the system: the subjacent two-dimensional Hilbert space is spanned by the two possible paths in the interferometer and the evolution of the state is controlled by phase shifters and absorbers. A related experiment was reported previously by some of the authors [1] to verify the *cyclic* spatial geometric phase. The interpretation of this experiment, namely to ascribe a geometric phase to this particular state evolution, has met severe criticism [2]. The extension to *non-cyclic* evolution manifests the correctness of the interpretation of the previous experiment by means of an explicit calculation of the non-cyclic geometric phase in terms of paths on the Bloch-sphere.

PACS numbers: 03.75.Dg, 03.65.Vf, 07.60.Ly, 61.12.Ld

Keywords: geometric phase; neutron interferometry

Discovered first by Pancharatnam [3] in the fifties a vast amount of intellectual work has been put into the investigation of geometric phases. In particular, Berry showed in 1984 [4] that a geometric phase arises for the adiabatic evolution of a quantum mechanical state which triggered renewed interest in this topic. The evolution of a system returning to its initial state causes an additional phase factor connected only to the path transversed in the state space. There have been several extensions in various directions [5, 6, 7, 8, 9, 10] for pure states, but also for the mixed state case [11, 12, 13]. Besides these theoretical work numerous experiments have been performed to verify geometric phases using various types of quantum mechanical systems, e. g. polarized photons [14] or NMR [18]. In addition, neutron interferometry has been established as a particularly suitable tool to study basic principles of quantum mechanics [19, 20, 21] providing explicit demonstrations [1, 15, 16] and facilitating further studies [17] of geometric phenomena.

There is no reason to consider only inherent quantum properties like spin and polarization for the emergence of a geometric phase; equally well one can consider a subspace of the momentum-space of a particle and its geometry. On this issue some authors of the present article performed an experiment to test the spatial geometric phase [1]. The results are fully consistent with the values predicted by theory, however, there is an ambiguity in the interpretation as pointed out by Wagh [2]. He concludes that in this setup the phase picked up by a state during its evolution is merely a U(1) phase factor stemming from the dynamics of the system and not due to the geometric nature of the subjacent Hilbert space. In his comment he refused the existence of a SU(2) state evolution necessary for a geometric phase factor.

In this paper we generalize the idea of the experiment in [1] to resolve the ambiguity in the interpretation of the latter neutron interferometry experiment. There the

geometric phase has been measured for a 2π (cyclic) rotation of the Bloch-vector representing the path state of the neutron. In order to deny Wagh's criticism we have measured the geometric phase for a rotation by an angle in the interval $[0, 2\pi]$ (non-cyclic) and – to show the applicability of the geometric phase concept – we have devised the path of the state vector on the Bloch-sphere to calculate the corresponding surface area enclosed by the evolution path. In the theory this surface area is proportional to the geometric phase, which has been determined experimentally to confirm the validity of our considerations and therefore the proper interpretation in terms of a geometric phase.

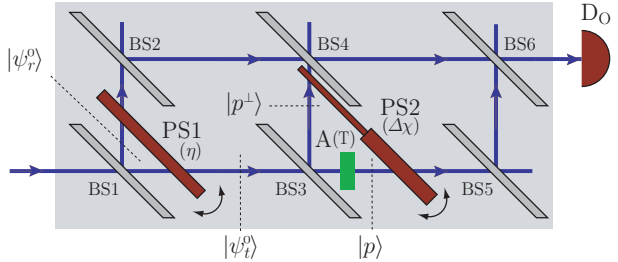


FIG. 1: Experimental setup utilizing a double-loop perfect-crystal neutron interferometer: One loop is used for the state manipulation with a phase shifter (PS2) together with a beam attenuator(A) and the other one provides a reference beam with adjustable phase by use of the phase shifter (PS1).

For testing the spatial geometric phase we use a double-loop interferometer (cf. Fig. 1), where the incident (unpolarized) neutron beam $|\psi\rangle$ is split at the beam splitter BS1 into a reflected beam $|\psi_r^0\rangle$ and a transmitted beam $|\psi_t^0\rangle$ before the beam splitter BS3, where $|p\rangle$

The reflected beam $|\psi_r^0\rangle$ is used as a reference with adjustable relative phase η to $|\psi_t^0\rangle$ due to the phase shifter PS1. The latter beam is defined to be in the state $|\psi_t^0\rangle \equiv |p\rangle$ before the beam splitter BS3, where $|p\rangle$

is the eigenstate to the operator $P_p = |p\rangle\langle p|$ measuring the path. Behind BS3 there are two possible orthogonal paths $|p\rangle$ and $|p^\perp\rangle$ spanning a two-dimensional Hilbert space, where $|p\rangle$ denotes the state of the transmitted beam and $|p^\perp\rangle$ the state of the reflected beam, respectively. Having a 50:50 beam splitter $|\psi_t^0\rangle$ is transformed into a superposition of the basis vectors $|p\rangle$ and $|p^\perp\rangle$: $|\psi_t^0\rangle \mapsto |q\rangle \equiv (|p\rangle + |p^\perp\rangle)/\sqrt{2}$. The corresponding projection operator $P_q \equiv |q\rangle\langle q| = (1 + |p\rangle\langle p^\perp| + |p^\perp\rangle\langle p|)/2$ (and also $P_{q^\perp} = 1 - P_q = |q^\perp\rangle\langle q^\perp|$) measures the interference instead of the paths.

The transmitted beam $|\psi_t^0\rangle$ is subjected to further evolution in the second loop of the interferometer by use of beam splitters (BS4, BS5 and BS6), an absorber (A) with transmission coefficient T and a phase shifter (PS2) generating a phase shift of $e^{i\chi_1}$ on the upper ($|p^\perp\rangle$) and $e^{i\chi_2}$ on the lower beam path ($|p\rangle$), respectively, yielding the final state $|\psi_t\rangle$. Thus, the evolution causing the spatial geometric phase can be written as

$$\begin{aligned} |\psi_t^0\rangle &\xrightarrow{\text{BS3}} \frac{1}{\sqrt{2}}(|p^\perp\rangle + |p\rangle) \xrightarrow{\text{A}} \frac{1}{\sqrt{2}}(|p^\perp\rangle + \sqrt{T}|p\rangle) \quad (1) \\ &\xrightarrow{\text{PS2}} \frac{1}{\sqrt{2}}(e^{i\chi_1}|p^\perp\rangle + \sqrt{T}e^{i\chi_2}|p\rangle) \equiv |\psi_t\rangle. \end{aligned}$$

The transformation of the reference beam $|\psi_r^0\rangle$ is given by $|\psi_r^0\rangle \mapsto e^{i\eta}|\psi_r^0\rangle \mapsto e^{i\eta}|p^\perp\rangle$, which follows from the fact that the path of $|\psi_r^0\rangle$ coincides with the path of the beam reflected at BS3 labeled by $|p^\perp\rangle$.

In the last step $|\psi_t\rangle$ and the reference beam are recombined at BS6 and detected in the forward beam at the detector D_O . This recombination can be described by application of the interference projection operator $P_q = |q\rangle\langle q|$ to $|\psi_t\rangle$ as well as to $|\psi_r^0\rangle$:

$$\begin{aligned} |\psi_t'\rangle &\equiv P_q|\psi_t\rangle = K(e^{i\chi_1} + \sqrt{T}e^{i\chi_2})|q\rangle \\ e^{i\eta}|\psi_r'\rangle &\equiv P_qe^{i\eta}|\psi_r^0\rangle = Ke^{i\eta}|q\rangle, \quad (2) \end{aligned}$$

where K is some scaling constant.

The intensity I measured in the detector D_O is proportional to the modulus squared of the superposition $|\psi_t'\rangle + e^{i\eta}|\psi_r'\rangle$:

$$\begin{aligned} I \propto & \ ||\psi_t'\rangle + e^{i\eta}|\psi_r'\rangle|^2 = \langle\psi_r'|\psi_r'\rangle + \langle\psi_t'|\psi_t'\rangle + \\ & + 2|\langle\psi_r'|\psi_t'\rangle| \cos(\eta - \Phi) \quad (3) \end{aligned}$$

with $\Phi \equiv \arg\langle\psi_r'|\psi_t'\rangle$. For our purposes a double loop interferometer is inevitable, since we measure the phase shift generated in one interferometer loop relative to the reference beam, in contrast to a phase difference between two paths measured in usual interferometric setups. Here, the beam $|\psi_r'\rangle$ provides a phase shift of η relative to $|\psi_t'\rangle$ enabling us to extract the additional phase $\arg\langle\psi_r'|\psi_t'\rangle$ from the interference pattern in Eq. (3).

Clearly, in the beam ending at the detector D_O “both the constituent subbeam states [...] are identical to the

incident state [...] in momentum, energy and spin,” as pointed out by Wagh [2]. This is due to the projection to the state $|q\rangle$ described by Eq. (2). Moreover, the relative phase difference between both subbeams provides information about the evolution of the state $|\psi_t^0\rangle$ in state space due to its manipulation with beam splitters, absorber and phase shifters. By removing the dynamical part we can measure the geometric phase. Explicitly we obtain

$$\Phi = \frac{\chi_1 + \chi_2}{2} - \arctan \left[\tan \left(\frac{\Delta\chi}{2} \right) \left(\frac{1 - \sqrt{T}}{1 + \sqrt{T}} \right) \right], \quad (4)$$

where $\Delta\chi \equiv \chi_2 - \chi_1$. The geometric phase Φ_g is defined as [8]

$$\Phi_g \equiv \Phi - \Phi_d, \quad (5)$$

where Φ_d denotes the dynamical part. The dynamical phase Φ_d stemming from the phase shifter PS2 is given by a sum of the phase shifts χ_1 and χ_2 weighted with the transmission coefficient T [1, 2], $\Phi_d = (\chi_1 + T\chi_2)/(1 + T)$. This quantity vanishes by an appropriate choice of phase shifts and transmission, i. e. $\Phi_d = 0$ for $\chi_1/\chi_2 = -T$.

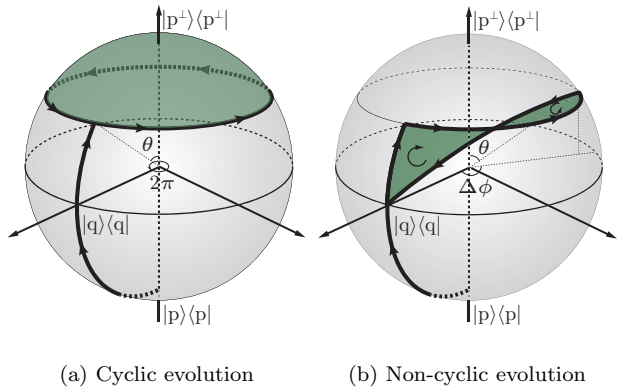


FIG. 2: Paths on the Bloch-sphere corresponding to the evolution of the state $|\psi_t^0\rangle$ (a) in the cyclic and (b) non-cyclic case. The enclosed solid angle as seen from the origin of the sphere is proportional to the geometric phase observed in the experiment.

The result from Eq. (4) can also be obtained by purely geometric considerations. Since we are dealing with a two-level system corresponding to the possible paths of $|\psi_t^0\rangle$ in the second loop of the interferometer the state space is equivalent to a sphere in \mathbb{R}^3 , known as the Bloch-sphere [22, 23, 24]. From theory we know that Φ_g defined in Eq. (5) can be calculated via the (oriented) surface area enclosed by the path of the state vector on the Bloch-sphere and proportional to the enclosed solid angle as seen from the origin of the sphere.

This representation is particularly useful to depict all possible states and their evolutions in a two-dimensional Hilbert space. To each point on the sphere there is a corresponding projection operator. Either the projection operators corresponding to path observables ($|p\rangle\langle p|$ and $|p^\perp\rangle\langle p^\perp|$) or to interference observables ($|q\rangle\langle q|$ and $|q^\perp\rangle\langle q^\perp|$) can be chosen as basis states. Here we have chosen the former so that the north and the south pole of the sphere are identified with the eigenstates of the observables $|p^\perp\rangle\langle p^\perp|$ and $|p\rangle\langle p|$, i. e. with orthogonal states with well known paths, as depicted in Fig. 2. At the beam splitter BS3 the state $|\psi_t^0\rangle$ originating from the point $|p\rangle\langle p|$ is projected to an equal superposition of upper path and lower path represented by a geodesic from the south pole to the equatorial line on the Bloch-sphere [26].

The absorber changes the weights of the superposed basis states $|p\rangle$ and $|p^\perp\rangle$ according to its transmittivity T which can be parameterized by the polar angle θ by setting $T = \tan^2 \theta/2$ with $\theta \in [0, \pi/2]$. For no absorption ($T = 1$ or $\theta = \pi/2$) the state stays on the equator of the Bloch-sphere. By inserting a beam block ($T = 0$ or $\theta = 0$) the state is pinned on the north pole, since there is no contribution to the intensity in D_O from the lower beam path. For $T \in (0, 1)$ the state is encoded as a point on the geodesic from the north pole to the equatorial line.

The phase shifter PS2 induces a relative phase shift between the superposing states of $\Delta\chi = \chi_2 - \chi_1$. This corresponds to an evolution along a circle of latitude on the Bloch-sphere with periodicity 2π . The recombination at BS5 followed by the detection of the forward beam in D_O is represented as a projection to the starting point on the equatorial line, i. e. we have to close the curve associated with the evolution of the state by a geodesic to the point $|q\rangle\langle q|$ in accordance to the results of Samuel and Bhandari [7].

This evolution path is depicted in Figs. 2(a) and 2(b) for cyclic and non-cyclic evolution, respectively. For a relative phase difference greater than $\pi/2$ we have to take the direction of the loops into account: In Fig. 2(b) the first loop is transversed clockwise, whereas the second loop is transversed counter-clockwise yielding a positive or negative contribution to the geometric phase, respectively.

The numerical calculation of the surface area F enclosed by the path transversed by the neutron is straightforward by evaluating the solid angle $\Omega = \int_F \sin \theta d(\Delta\chi) d\theta$ via a surface integral and using the relation $\Phi_g = -\Omega/2$ [4]. For the cyclic case this integral can be solved easily to obtain $\Phi_g = \pi(\cos \theta - 1)$. For the non-cyclic case no analytic expression has been found. However, the results based on Eq. (4) are equal to the results obtained numerically for Ω from the integral above. This substantiates the emergence of a geometric phase in this type of experiment contrary to other claims [2].

As for the experimental demonstration we have used

the double-loop perfect-crystal-interferometer installed at the S18 beamline at the high-flux reactor ILL, Grenoble [25]. A schematic view of the setup is shown in Fig. 1. Before falling onto the skew-symmetric interferometer the incident neutron beam is collimated and monochromatized by the 220-Bragg reflection of a Si perfect crystal monochromator placed in the thermal neutron guide H25. The wavelength is tuned to give a mean value of $\lambda_0 = 2.715\text{\AA}$ and prism-shaped silicon wedges are put between the collimator and the interferometer. The refraction at these components enables us to get rid of the higher harmonics by tuning the angle of the interferometer adequately. The beam cross-section is confined to $5 \times 5\text{mm}^2$ and by use of an isothermal box enclosing the interferometer thermal environmental isolation is achieved. As phase shifters parallel sided aluminium plates are used. In fact, a 5mm-thick plate is taken for the first phase shifter (PS1) inserted in the former loop and plates of different thickness ($d_1 = 0.5\text{mm}$ and $d_2 = 4.1\text{mm}$) are used as the second phase shifter (PS2). The different thicknesses together with a specific choice of the absorber (A) are to eliminate a phase of unwanted dynamical origin. Such a pair of phase plates for the PS2 yields a ratio of $d_1/d_2 = 0.5/4.1 = 0.122$ for $-\chi_1/\chi_2$. When the absorber is chosen so that the condition $T_2/T_1 = -\chi_1/\chi_2$ (T_j is the transmission coefficient of each beam after PS2 and A) is fulfilled, all dynamical phase contributions vanish. For an appropriate adjustment of the transmission coefficient, we use a gadolinium solution as absorber, which is tuned to exhibit a transmissivity of $T_{\text{abs}} = 0.118(5)$. Taking the absorption of the 0.5mm Al phase shifter into account, a ratio $T_2/T_1 = 0.120(5)$ is realized.

The phase shifts Φ of the sinusoidal intensity modulations due to PS1 are determined at various points on the path traced out by the state, corresponding to a non-cyclic evolution. In practice, this is achieved by measuring the intensity modulation by PS1 at various positions of the PS2 [1]. The parameter of the evolution is the relative phase shift $\Delta\chi = \chi_2 - \chi_1$, which was varied from -0.2π to 3.0π . The measured phase shift is plotted as the function of $\Delta\chi$ in Fig. 3 together with theoretically predicted curves: one (dotted curve) is obtained by assuming an ideal situation of hundred percent visibility, whereas the practically diminished visibility is taken into account for the other (solid curve). In particular, the two subbeams from the second loop are only partially overlapping (in space) with the reference beam at BS6 due to unequal spatial displacements caused by the unequal thicknesses of the plates of PS2. These non-overlapping parts do not contribute to the interference pattern that in turn induces a flattening of the measured curve relative to the ideal curve. The solid line is obtained from a least-squares fit to the measured data using the function $\arg[\sqrt{T_1}e^{-is_1\Delta\chi} + C\sqrt{T_2}e^{is_2\Delta\chi}]$ with $s_{1,2} = d_{1,2}/(d_1+d_2)$. This is a version of Eq. (4) adapted to the experimental

situation with the fit coefficient C calculated to $0.57(2)$ reflecting the different contrasts of the two subbeams generated at BS3 with the reference beam. Note, that this does not invalidate the discussion on the vanishing dynamical phase, since the deviation of the experimentally determined (solid) curve from the ideal (dotted) curve is only due to the measurement circumstances in the neutron interferometer. The contribution of the dynamical phase due to the slightly different ratios of χ_1/χ_2 and T_2/T_1 can be calculated to yield corrections of the order $\pm 2 \times 10^{-2}$.

One can recognize the increase of the measured phase shift Φ in Fig. 3 due to the positively oriented surface on the Bloch-sphere (c.f. Fig. 2(b)) followed by a decrease from counter-clockwise transversed loop yielding a negative phase contribution. This behaviour clearly exhibits the geometric nature of the measured phase. For a cyclic evolution ($\Delta\chi = 2\pi$) the measured geometric phase is $-0.684(48)$ which is in a good agreement with the analytical value -0.683 for a ratio $\chi_1/\chi_2 = T_2/T_1 = 0.5/4.1$. Measurements of other T -values are also of interest and will be issue of a forthcoming publication.

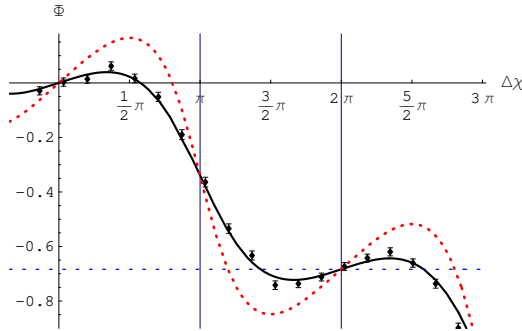


FIG. 3: Observed phase shift Φ for a non-cyclic evolution of the state vector parameterized by the relative phase shift $\Delta\chi$. The dotted line indicates the theoretical prediction for the geometric phase assuming hundred percent visibility, whereas the solid line takes the diminished visibility into account. For a cyclic evolution ($\Delta\chi = 2\pi$) we obtain $\Phi_g = -0.684(48)$ radians for the transmission ratio $T_2/T_1 = 0.120$.

In summary we have shown that one can ascribe a geometric phase not only to spin evolutions of neutrons, but also to evolutions in the spatial degrees of freedom of neutrons in an interferometric setup. This equivalence is evident from the description of both cases via state vectors in a two dimensional Hilbert space. However, there have been arguments contra the experimental verification in [1] which we believe can be settled in favour of a geometric phase appearing in the setup described above. The twofold calculations of the geometric either in terms of a shift in the interference fringes or via surface integrals in an abstract state space allows for a geometric interpretation of the obtained phase shift. The experiments exhibit a shift of the interference pattern that reflects these the-

oretical predictions up to influences due to the different visibilities in the different beams.

This research has been supported by the Austrian Science Foundation (FWF), Project Nr. F1513. S. F. wants to thank E. Sjöqvist for valuable discussions and K. Durstberger for critical readings of the manuscript.

* Electronic address: sfilipp@ati.ac.at
 † Electronic address: hasegawa@ati.ac.at

[1] Y. Hasegawa, M. Zawisky, H. Rauch, and A. I. Ioffe, Phys. Rev. A **53**, 2486 (1996).
 [2] A. G. Wagh, Phys. Rev. A **59**, 1715 (1999).
 [3] S. Pancharatnam, Proc. Indian Acad. Sci., Sect. A **44**, 247 (1956).
 [4] M. V. Berry, Proc. R. Soc. Lond. A **392**, 45 (1984).
 [5] F. Wilczek and A. Zee, Phys. Rev. Lett. **52**, 2111 (1984).
 [6] Y. Aharonov and J. Anandan, Phys. Rev. Lett **58**, 1593 (1987).
 [7] J. Samuel and R. Bhandari, Phys. Rev. Lett. **60**, 2339 (1988).
 [8] N. Mukunda and R. Simon, Ann. Phys. **228**, 205 (1993).
 [9] A. K. Pati, J. Phys. A **28** 2087(1995).
 [10] N. Manini and F. Pistolesi, Phys. Rev. Lett. **85**, 3067 (2000).
 [11] A. Uhlmann, Rep. Math. Phys. **24** 229 (1986).
 [12] E. Sjöqvist, A. K. Pati, A. Ekert, J. S. Anandan, M. Ericsson, D. K. L. Oi, and V. Vedral, Phys. Rev. Lett. **85**, 2845 (2000).
 [13] S. Filipp and E. Sjöqvist, Phys. Rev. Lett. **90** 050403(2003).
 [14] A. Tomita and R. Y. Chiao, Phys. Rev. Lett. **57**, 937 (1986).
 [15] T. Bitter and D. Dubbers, Phys. Rev. Lett. **59**, 251 (1987).
 [16] Y. Hasegawa, R. Loidl, M. Baron, G. Badurek, and H. Rauch, Phys. Rev. Lett. **87**, 070401 (2001); Y. Hasegawa, R. Loidl, G. Badurek, M. Baron, N. Manini, F. Pistolesi, and H. Rauch, Phys. Rev. A **65**, 052111 (2002).
 [17] R. A. Bertlmann, K. Durstberger, Y. Hasegawa, and B. C. Hiesmayr, Phys. Rev. A **69**, 032112 (2004).
 [18] J. Du, P. Zou, M. Shi, L. C. Kwek, J.-W. Pan, C. H. Oh, A. Ekert, D. K. L. Oi, and M. Ericsson, Phys. Rev. Lett. **91**, 100403 (2003).
 [19] H. Rauch and S. A. Werner, *Neutron Interferometry: Lessons in experimental Quantum Mechanics* (Clarendon Press, Oxford, 2000).
 [20] Y. Hasegawa, R. Loidl, G. Badurek, M. Baron, and H. Rauch, Nature **425**, 45 (2003).
 [21] H. Rauch, H. Lemmel, M. Baron, and R. Loidl, Nature **417**, 630 (2002).
 [22] P. Mittelstaedt, A. Prieur, and R. Schieder, Found. Phys. **17**, 891 (1987).
 [23] P. Busch, Found. Phys. **17**, 905 (1987).
 [24] Y. Hasegawa and S. Kikuta, Z. Phys. B **93**, 133 (1994).
 [25] M. Zawisky, M. Baron, R. Loidl, and H. Rauch, Nucl. Instr. Meth. A **481**, 406 (2002).
 [26] The particular point on the equator is arbitrary due to the arbitrary choice of the phases of the basis vectors.